Improvement of Line Stability Indices with Solar Photovoltaic Integration in Power System Network

Santosh Kumar Gupta[1†], **Vikash Kumar**[2], **Kanchan Bala**[3], **Shahzad Ahsan**[4], **Ashwini Tiwari**[5], **Zafar Ayub Ansari**[6], **Dhananjay Kumar**[1], **Ashish Ranjan**[7], and **Arjun Kumar**[8], Non-members

ABSTRACT

The stability of power systems is challenged by the rise of renewable energy sources, fast load changes, and increased consumption. The voltage stability index (VSI) is crucial for assessing power supply stability and triggering responses to voltage instability. This paper uses fast voltage stability index (FVSI), line stability factor (Lqp), and line stability index (Lmn) to evaluate the IEEE 14-bus and 118-bus systems. With solar photovoltaic generator (SPVG) integration at the most critical bus, these indices assess system stability under nominal and varied reactive power conditions. The main goal of the paper is to mitigate critical line severity by integrating PV systems, using Newton-Raphson load flow analysis in PSAT/MATLAB. Results show significant improvements in line indices with SPVG, notably reducing critical line severity for the IEEE 14-bus (lines 5-1) and 118-bus (lines 44-43) systems.

Keywords: Critical line, Indices, Load flow, Stability, Solar PV generation

1. INTRODUCTION

Voltage stability is the capacity of a power system to maintain a consistent voltage at every bus throughout a disturbance [1]. One of the main concerns in the design and functioning of the power system has been identified as the possibility of voltage instability in the power system networks [2]. This happens because of problems with the economy and environment in addition to an increase in load demand. They primarily arise from the stress placed on the present power system, which could cause it to be near its stability limit [3]. A voltage collapse is a sequence of events that happens after all preventive measures have been taken. A significant portion of the power system eventually goes black as a result of this series of events, causing a gradual decline in voltage [4]. This usually occurs during large interruptions or in areas of the network because reactive power is limited. There has been a lot of study done on improving the voltage stability of the power system, and various solutions, including load shedding, active power control, and VAR (Volt Ampere Reactive) adjustment, have been successfully implemented. Numerous previous works for undervoltage and underfrequency exist, but none of them offer a solution for the power flow equations. A load shedding strategy known as optimal steady state was developed to reduce the sum of squares of the power differentials [5]. The model considered the transferred energy as a conditional variable quantity that varied according to the magnitude of the bus voltage. A method of load shedding was presented in [6] with the goal of minimizing system loss with restrictions on generator limits and line flow limitations in order to minimize load shedding in the scenario when total generation is less than total demand.

In specified conditions, voltage stability indices serve to assess a long-term development trend, forecast future modifications to the structure of the power system, and place the current operation of the system in context. In [7], the L-indicator index was used to create a novel, simplified method for determining the optimum location and amount of load to shed in order to keep the system voltage from entering the unstable zone. The power stability index (PSI) is suggested in [8] to provide the best possible distribution of distributed generation (DG) near voltage collapse within a critical sensitive bus. The

Manuscript received on June 15, 2025; revised on August 10, 2025; accepted on August 14, 2025. This paper was recommended by Associate Editor Chawasak Rakpenthai.

[1]The author is with Department of Electrical Engineering, Government Engineering College, Siwan, Bihar – 841226, India.

[2]The author is with Department of Electrical and Electronics Engineering, Rashtra Kavi Ramdhari Singh Dinkar College of Engineering, Begusarai, Bihar – 851134, India.

[3]The author is with Department of Computer Science and Engineering, Gaya College of Engineering, Gaya, Bihar – 823003, India.

[4]The author is with Department of Electrical Engineering, Muzaffarpur Institute of Technology, Muzaffarpur, Bihar – 842003, India.

[5]The author is with Department of Civil Engineering, L.D.A.H. Rajkiya Engineering College, Mainpuri, Uttar Pradesh – 205119, India.

[6]The author is with Department of Electrical and Electronics Engineering, Loknayak Jai Prakash Institute of Technology, Chhapra, Bihar –841302, India.

[7]The author is with Department of Electrical and Electronics Engineering, Nalanda College of Engineering, Chandi (Nalanda), Bihar – 803108, India.

[8]The author is with Department of Electrical Engineering, Shri Phanishwar Nath Renu Engineering College, Araria, Bihar – 854318, India.

[†]Corresponding author: santoshgupta1990@gmail.com

Digital Object Identifier: 10.37936/ecti-eec.2525233.259359

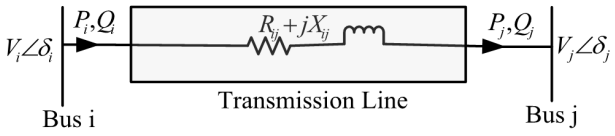

***Fig. 1**: Two bus system with line parameters.*

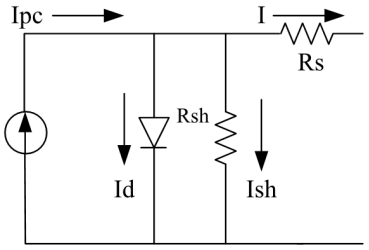

***Fig. 2**: Generator model of PV module.*

VDI index can be broadly applied to an N-bus system by considering the total of N voltage variations. In [9], power flow analysis and composite load modelling are taken into account to create a new index called the stability index (SI) for radial distribution topology. The Voltage Collapse Prediction Index (VCPI) was developed in [10] to forecast voltage collapse in a power system. The system variables, including the system admittance matrix, voltage angle data, and bus voltage magnitude, are used to calculate this index. The voltage collapse concept was the basis for the bus participation factor (BPF) indices presented by the authors in [11]. One of the measures used to identify the weakest node in a system is the bus participation factor. According to system variable factors (bus voltage and current magnitudes), the voltage stability index (VSI) is driven in [13] to determine the stability margin point. The Equivalent Node Voltage Collapse Index (ENVCI) is presented in [12] using the equivalent system model (ESM). This index corresponds to several benefits, including effectiveness from the outside the local network and the local network, real-time application, and voltage collapse point calculation. Taylor's theorem was used to calculate the voltage collapse index (VCI) in [13] based on the apparent power change of a system. A two-bus power flow with a zero threshold at the stable point is used in [14] to calculate the voltage stability factor (VSF). Using power transfer concepts, the line stability index (Lmn) is introduced in [15]. The line stability factor (Lqp) is presented in [16] using line flow data. Fast voltage stability index (FVSI) was introduced in [17]. A study [18] uses the provided L-index and the minimal eigenvalue of a reduced Jacobian matrix to suggest a composite voltage stability index (CVSI) that minimizes the voltage stability of the system. Five voltage stability indices (VSIs) are compared in research [19] for their efficacy under optimal power flow.

Two composite stability indices and a probabilistic framework are presented in the research [20] for the simultaneous assessment of many power system stability issues. The loadability margin, which serves as a stand-in for the margin of sustained voltage stability, is predicted using machine learning (ML) in [21]. In [22], the equilibrium between heat absorption and dissipation for conductors above ground is used to describe the electrothermal coupling effect in a single power flow model. In order to solve single-objective OPF (SOOPF), multi-objective OPF (MOOPF), and many-objective OPF (MaOPF) problems, [23] introduces the many-objective marine predators algorithm (MaMPA) to solve a variety of other problems, with the exception of MaOPF problems. In research [24], a novel approach for solving many-objective optimal power flow (MaOOPF) issues is proposed: two-archive Harris Hawk optimisation (TwoArchHHO). The reactive power mismatch between generation and demand is the cause of the voltage stability problem. Rearranging the reactive power generation or giving the system more reactive support are two ways to meet the reactive power demand [25]. Since the transmission system has gained flexibility, the Flexible AC Transmission System (FACTS) is able to control the reactive power flow in a more dynamic manner [26]. Renewable Energy (RE) integration with the electric power grid can also overcome voltage stability problems. Solar energy, wind power, and biomass are examples of popular renewable energy sources. Among these, solar energy has drawn the most attention because of its low installation costs and potential for significant energy gains. Although integrating solar PV into the power system may be a way to address the problems of fossil fuel scarcity and pollution in the environment. Doing so may also bring up a number of technical challenges (such as power quality, power system stability, operation and control, and so on) because the network design did not initially take solar PV integration into account [27]. Many researchers have made it their main objective to investigate how solar PV installations affect transmission and/or distribution networks [27], [28], [29]. In [30], two sensitivity indices have been used to evaluate the voltage sensitivities of buses to an increase in RE penetration. Paper [31] proposes a modified Sobol's approach sensitivity analysis to identify the critical parameters in the utility-scale solar PV plant model. In order to investigate and assess the power systems' voltage stability with rising levels of PV penetration, the paper [32] uses modal analyses of both the PV and QV power systems. The research [33] proposes a data-driven integrated framework to enhance VSM of the grid with a PV system.

In this paper, the line stability indices Lqp, FVSI, and Lmn of all lines of the IEEE 14-bus and IEEE 118-bus systems have been calculated with and without the presence of the solar photovoltaic system. The critical line is predicted based on the index value near unity. The solar system has been integrated with critical buses of the system to improve the severity of the lines. The line stability indices of the lines have been compared with and without ok integration of the solar photovoltaic system under four types of loading scenarios. The severity of the

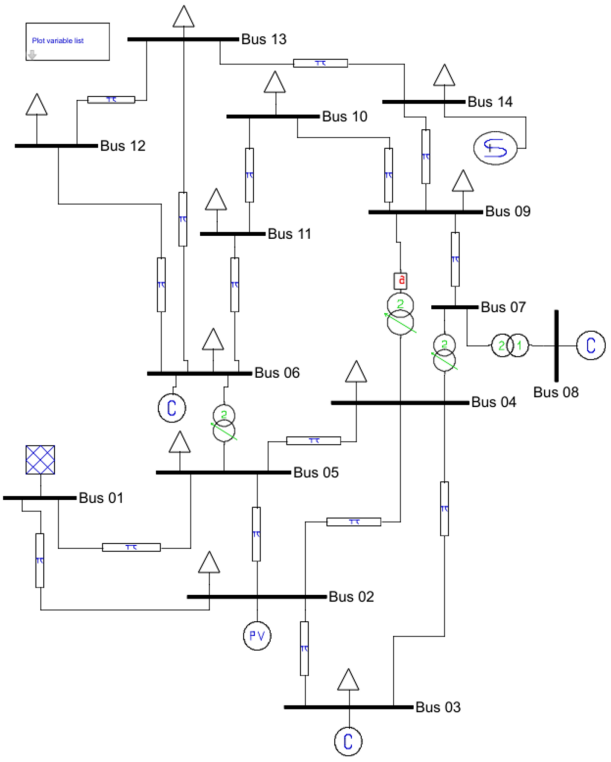

***Fig. 3**: IEEE-14 bus network.*

most critical lines of the IEEE 14-bus and IEEE 118-bus systems have been reduced after the integration of the solar PV system at most appropriate locations.

2. LINE STABILITY INDICES

Due to the scarcity of natural resources, power system operators are always trying to utilise their maximum limits. Consequently, the power system operates at its maximum operating limits. In this satuation, there is always a high risk of failure of the whole system under any abnormal circumstances. So, there is always a requirement for proper continuous monitoring, so that preventive actions can be taken before the collapse of the system. Line stability indices were developed to monitor the severity of the power system lines. Generally, all line stability indices are represented by a mathematical equation that depends upon the line parameters and line flow data. The values of these indices vary from zero to one. One or near One value indicates the most severe situation, whereas a near-zero value indicates a highly stable system. In this Paper, three line stability namely: Lmn/FVSI/Lqp, are used to calculate the criticalness of the lines. For a two-bus system as shown in Fig. 1, these are explained as:

2.1 Line Stability Index (Lmn)

Researchers have commonly utilised the line stability index, or Lmn, to specify each line's stability criterion [15]. It is written as follows:

$$L_{mn} = \frac{4X_{ij}Q_j}{\left(V_i \sin(\theta_{ij} - \delta)\right)^2} \tag{1}$$

where, $\theta_{ij}$and$X_{ij}$are the line impedance angle and line reactance between bus i and bus j, respectively; V_i and $Q_j$are sending the end bus voltage magnitude and the receiving end reactive power, respectively; $\delta = \delta_i - \delta_j$ for the two bus systems.

2.2 Fast Voltage Stability Index (FVSI)

The critical line is also selected based on a line's FVSI value, which is mathematically defined as [17]:

$$FVSI = \frac{4\left|Z_{ij}\right|^2 Q_j}{V_i X_{ij}} \tag{2}$$

where, Z_{ij} is the line impedance between bus i and bus j.

2.3 Line Stability Factor (Lqp)

The critical line can also be found using the line stability factor, which is described in terms of real and reactive power as follows [16]:

$$Lqp = 4\left(\frac{X_{ij}}{V_i^2}\right)\left(\frac{X_{ij}}{V_i^2}P_i^2 + Q_j\right) \tag{3}$$

The severity of the lines can be decided by an index, Lmn/FVSI/Lqp.

3. SOLAR PHOTOVOLTAIC GENERATION

A device that directly converts solar radiation into electrical energy is called a photovoltaic cell. In addition,

***Table 1**: Line data of IEEE-14 bus system.*

Line No.	From bus	To bus	Line Imp. Angle (Θ) (in degrees)	Line Reactance (x)	Line Resistance (r)
1	5	4	72.4100	0.0421	0.0134
2	1	2	71.8648	0.0592	0.0194
3	9	10	69.3712	0.0845	0.0318
4	7	9	90.0000	0.1100	0.0000
5	6	13	63.0789	0.1303	0.0662
6	3	4	68.6046	0.1710	0.0670
7	2	5	71.8651	0.1739	0.0570
8	8	7	90.0000	0.1762	0.0000
9	2	4	71.7593	0.1763	0.0581
10	11	10	66.8684	0.1921	0.0821
11	3	2	76.6474	0.1980	0.0470
12	6	11	64.4743	0.1989	0.0950
13	12	13	42.1376	0.1999	0.2209
14	4	7	90.0000	0.2091	0.0000
15	5	1	76.3828	0.2230	0.0540
16	5	6	90.0000	0.2520	0.0000
17	6	12	64.3369	0.2558	0.1229
18	9	14	64.8210	0.2704	0.1271
19	14	13	63.8420	0.3480	0.1709
20	4	9	90.0000	0.5562	0.0000

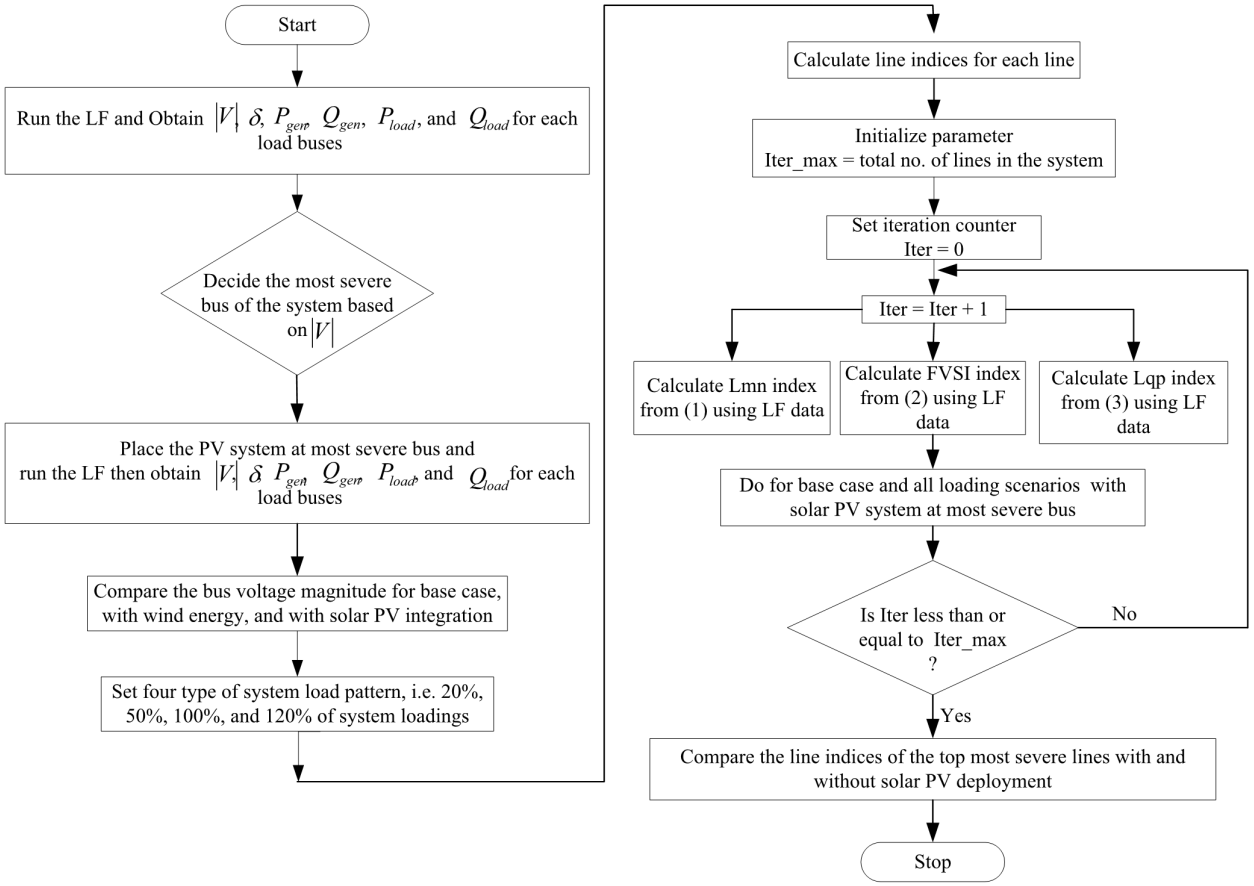

***Fig. 4**: Flow chart representation of the proposed approach.*

***Table 2**: Line stability indices with and without deployment of the solar PV system at loading multiplier k=0.2.*

Lines		Line stability indices (in p.u.) at k=0.2					
From Bus	To Bus	Without PV integration			With PV integration		
		Lmn Indices	FVSI Indices	Lqp Indices	Lmn Indices	FVSI Indices	Lqp Indices
5	**1**	**0.9914**	**1.0153**	**0.9458**	**0.9814**	**0.9718**	**0.8036**
3	**4**	**0.918**	**0.9503**	**0.9215**	**0.9118**	**0.9217**	**0.9168**
3	**2**	**0.8146**	**0.8758**	**0.9975**	**0.7936**	**0.7446**	**0.8737**
2	**4**	**0.7159**	**0.2372**	**0.8584**	**0.6435**	**0.1204**	**0.8559**
8	**7**	**0.677**	**0.677**	**0.677**	**0.6248**	**0.6248**	**0.6248**
5	4	0.6404	0.533	0.3379	0.2916	0.5108	0.3369
14	13	0.6202	0.6749	0.4356	0.4765	0.4459	0.3564
2	5	0.4978	0.2779	0.8461	0.4561	0.2534	0.8324
6	11	0.3437	0.3295	0.2906	0.3008	0.2861	0.2568
9	14	0.3419	0.2881	0.1685	0.2719	0.2801	0.2085
11	10	0.338	0.3316	0.2918	0.2877	0.2812	0.2486
4	7	0.3156	0.2627	0.2033	0.2621	0.184	0.1357
5	6	0.1963	0.0985	0.5045	0.1803	0.0885	0.3016
6	13	0.1668	0.1513	0.1602	0.1392	0.131	0.1227
9	10	0.1603	0.1565	0.1357	0.1228	0.1197	0.1028
1	2	0.1317	0.1269	0.1202	0.2294	0.0903	0.1088
12	13	0.0869	0.0852	0.0399	0.0853	0.084	0.035
6	12	0.0771	0.071	0.0856	0.0762	0.0705	0.0801
7	9	0.0478	0.0461	0.1751	0.0408	0.0418	0.1269
4	9	0.0051	0.0034	0.0864	0.3411	0.2663	0.076

this module is made up of many cells that are connected in series and parallel to determine the voltage and current values based on the photovoltaic effect. A semiconductor called a photovoltaic cell is made up of a pn junction diode, which is capable of producing electrical energy when exposed to photons from sunshine [34]. Aside from the problem of global warming and the depletion of fossil fuels, solar cells have just lately been commercially

***Table 3**: Line stability indices with and without deployment of the solar PV system at loading multiplier k=0.5.*

Lines		Line stability indices (in p.u.) at k=0.5					
From Bus	To Bus	Without PV integration			With PV integration		
		Lmn Indices	FVSI Indices	Lqp Indices	Lmn Indices	FVSI Indices	Lqp Indices
5	**1**	**0.9924**	**1.0161**	**0.9692**	**0.9816**	**0.9725**	**0.8297**
3	**4**	**0.923**	**0.9625**	**0.9238**	**0.8972**	**0.9582**	**0.9184**
14	**13**	**0.9022**	**0.9836**	**0.6426**	**0.7253**	**0.8672**	**0.5346**
3	**2**	**0.8215**	**0.8865**	**1.0029**	**0.7972**	**0.8615**	**0.8849**
2	**4**	**0.7314**	**0.2776**	**0.8627**	**0.6449**	**0.2544**	**0.8607**
8	7	0.7278	0.7278	0.7278	0.6809	0.6809	0.6809
5	4	0.6501	0.557	0.339	0.6224	0.5239	0.3359
2	5	0.5219	0.2926	0.8531	0.4777	0.2662	0.8393
6	11	0.4349	0.4198	0.3669	0.4002	0.383	0.339
11	10	0.4266	0.4199	0.3694	0.3804	0.3726	0.3292
9	14	0.3537	0.2943	0.1697	0.2891	0.2851	0.1358
4	7	0.3247	0.2946	0.2502	0.3155	0.2872	0.2136
6	13	0.2435	0.2223	0.2182	0.2203	0.2091	0.1853
5	6	0.2155	0.1056	0.6741	0.1836	0.0949	0.1893
9	10	0.1765	0.1721	0.1491	0.132	0.1285	0.1102
1	2	0.1581	0.1619	0.1399	0.1348	0.1583	0.1202
7	9	0.1555	0.1494	0.2886	0.1446	0.1308	0.2438
6	12	0.1265	0.1169	0.1239	0.1126	0.1044	0.1219
12	13	0.1263	0.1246	0.0581	0.1237	0.1113	0.0562
4	9	0.0462	0.0563	0.3421	0.0389	0.0541	0.0749

***Table 4**: Line stability indices with and without deployment of the solar PV system at loading multiplier k=1.0.*

Lines		Line stability indices (in p.u.) at k=1.0					
From Bus	To Bus	Without PV integration			With PV integration		
		Lmn Indices	FVSI Indices	Lqp Indices	Lmn Indices	FVSI Indices	Lqp Indices
5	**1**	**0.9931**	**1.0218**	**0.9762**	**0.9821**	**0.9898**	**0.8931**
3	**4**	**0.9325**	**0.9712**	**0.9273**	**0.9276**	**0.97**	**0.9104**
14	**13**	**0.9256**	**0.9875**	**0.6952**	**0.9021**	**0.9801**	**0.6511**
3	**2**	**0.8347**	**0.9671**	**1.0034**	**0.8256**	**0.9541**	**0.9253**
8	**7**	**0.8184**	**0.8184**	**0.8184**	**0.7816**	**0.7816**	**0.7816**
2	4	0.7917	0.3213	0.8703	0.7239	0.2348	0.8689
5	4	0.6722	0.5898	0.3394	0.659	0.5421	0.3299
11	10	0.601	0.5961	0.5262	0.5643	0.5552	0.4931
6	11	0.5943	0.5811	0.5051	0.5738	0.5553	0.488
2	5	0.5728	0.3252	0.8669	0.5215	0.2931	0.8518
9	14	0.3947	0.3165	0.1916	0.3539	0.3018	0.1853
4	7	0.3861	0.3212	0.5739	0.3152	0.2071	0.2686
6	13	0.3765	0.3478	0.3217	0.3595	0.3467	0.2959
7	9	0.3677	0.3478	0.5127	0.3594	0.337	0.4752
5	6	0.3658	0.1155	0.7162	0.3232	0.1051	0.1006
9	10	0.2235	0.2167	0.1876	0.1575	0.1526	0.1306
6	12	0.2119	0.1967	0.1912	0.2247	0.1823	0.1849
1	2	0.1685	0.2159	0.1555	0.1489	0.2015	0.1513
12	13	0.1303	0.2028	0.0942	0.1206	0.195	0.092
4	9	0.1005	0.0821	0.761	0.0942	0.0795	0.4604

available. The energy they generate is also incredibly affordable because solar energy is free [35]. The PV module's temperature and irradiance have an impact on how much power the system produces, as shown in Fig. 2 [36].

Monocrystalline silicon photovoltaic cells have a relatively high conversion efficiency of 15–20%. The protection of sunlight is thus achieved; however, this kind of panel malfunctions and loses efficiency [37]. In addition to the drawbacks, this panel will have a lot of empty space since solar cells with this shape—which are round or hexagonal—have a low density. Manufacturers typically use cutting techniques to create square shapes, but the production process inevitably results in higher losses, which raises the price.

4. RESULTS AND DISCUSSION

4.1 IEEE 14-Bus System

The proposed method for the assessment of the voltage stability has been investigated and validated on the standard IEEE 14-bus system [38]. The system is frequently utilised as a case study for a variety of research projects, including interconnected grid issues, load flow studies, and short circuit analysis. Fig. 2 illustrates the configuration of the IEEE 14-bus system. The resistances and reactances of the lines have been listed in Tab. 1.

***Table 5**: Line stability indices with and without deployment of the solar PV system at loading multiplier k=1.2.*

Lines		Line stability indices (in p.u.) at k=1.2					
From Bus	To Bus	Without PV integration			With PV integration		
		Lmn Indices	FVSI Indices	Lqp Indices	Lmn Indices	FVSI Indices	Lqp Indices
5	**1**	**0.9946**	**1.0225**	**0.9823**	**0.9932**	**0.9982**	**0.9292**
3	**4**	**0.9436**	**0.97512**	**0.9307**	**0.9326**	**0.9612**	**0.9208**
14	**13**	**0.9326**	**0.9884**	**0.745**	**0.9281**	**0.9871**	**0.6945**
3	**2**	**0.8516**	**0.9698**	**1.0078**	**0.8413**	**0.96**	**0.9837**
8	**7**	**0.8219**	**0.8219**	**0.8219**	**0.8205**	**0.8165**	**0.8105**
2	4	0.8054	0.3303	0.8794	0.601	0.2003	0.8724
5	4	0.7153	0.5926	0.3452	0.6363	0.5268	0.3246
11	10	0.6384	0.633	0.5609	0.6246	0.625	0.5563
6	11	0.6296	0.6169	0.5368	0.6092	0.6011	0.5255
2	5	0.5886	0.3274	0.8774	0.5442	0.3077	0.8576
7	9	0.4488	0.424	0.5828	0.4315	0.4209	0.5802
5	6	0.4426	0.1589	0.9331	0.4216	0.145	0.8533
4	7	0.4374	0.3998	0.6138	0.4305	0.3508	0.5219
9	14	0.4283	0.3628	0.2127	0.4121	0.3504	0.2025
6	13	0.4163	0.3863	0.3531	0.4088	0.3678	0.3443
4	9	0.3341	0.2101	0.8478	0.0981	0.0714	0.6804
9	10	0.2423	0.2261	0.1984	0.1756	0.1697	0.1449
6	12	0.2394	0.2227	0.2129	0.2337	0.2099	0.2063
12	13	0.2261	0.2267	0.1054	0.223	0.2163	0.1017
1	2	0.1716	0.2465	0.1762	0.1645	0.2415	0.1428

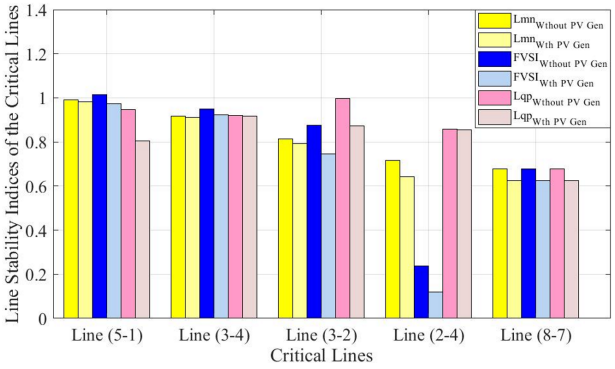

***Fig. 5**: Bar graph of the line stability indices of the most severe lines at loading multiplier k=0.2.*

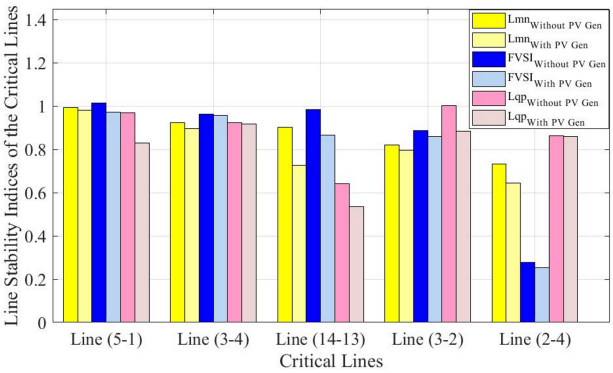

***Fig. 6**: Bar graph of the line stability indices of the most severe lines at loading multiplier k=0.5.*

***Table 6**: IEEE 14-bus, IEEE 118-bus, and PV systems parameters.*

System parameters	**IEEE 14-bus (in p.u.)**	**IEEE 118-bus (in p.u.)**
PSAT version used for simulation	2.1.11	
Solar PV generator (PV)	40 MW	100 MW
Total real power generation	7.610424	151.6911
Total loads of real power	6.143219	124.3596
Total generation of reactive power	7.655304	208.893
Total loads of reactive power	1.930726	50.56763

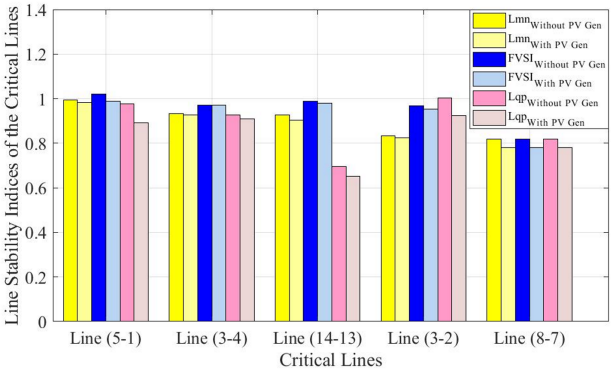

***Fig. 7**: Bar graph of the line stability indices of the most severe lines at loading multiplier k=1.0.*

The line impedance angles of all lines of the IEEE 14-bus system are calculated and listed in Tab. 1.

Three line indices, namely Lmn, FVSI, and Lqp, are used to evaluate the stability of the lines. There are four

types of reactive load (k=0.2, 0.5, 1.0, and 1.2) of the system that have been considered to examine the impact of the solar PV integration with the system. Under consideration of four types of reactive load variations, the voltage stability assessment of the system has been done as follows:

4.1.1 Line Stability Indices under PV integration with k=0.2

In the existing literature [39], for the IEEE 14-bus system, bus number 14 was decided as the most severe bus of the system. So, for the deployment of the compensating devices in the IEEE 14-bus system, this bus can be chosen as the most appropriate location. The solar PV generation system has been deployed at bus number 14 for the enhancement of the line voltage stability of the system. Line stability indices Lmn, FVSI, and Lqp for all lines of the test system have been calculated from Eqs. (1), (2), and (3), respectively, using Newton-Raphson load flow data for 'k=0.2' obtained from MATLAB/PSAT as listed in Tab. 2. From this table, it is observed that under the base case, the value of all indices of the lines (5-1), (3-4), (3-2), (2-4), and (8-7) are very high. So, these lines can be considered the most severe lines. Figure 4 shows the flow chart representation of the proposed methodology.

Also, it is observed that the value of the FVSI index for line (5-1) is beyond unity, which indicates a critical condition of this line. After the deployment of the solar PV generation system with the system the line indices are again calculated using Eqs. (1)-(3) with 'k=0.2', which are listed in Table 2. From this table, it is seen that the Lmn/FVSI/Lqp indices of the most severe line (5-1) get improved from 0.9914 p.u. to 0.9814 p.u., from 1.0153 p.u. to 0.9718 p.u., and from 0.9458 p.u. to 0.8036 p.u., respectively. The bar graph of the line stability indices of the top five severe lines at loading multiplier k=0.2 has been shown in Fig. 5.

4.1.2 Line Stability Indices under PV integration with k=0.5

The line stability indices are also calculated with and without deploying the solar PV generation system in the system at reactive power loading multiplier 'k=0.5'. For this loading scenario, at bus number 14, a solar PV generation system has been installed to improve the system's line voltage stability. For every line in the IEEE 14-bus system, the line stability indices Lmn, FVSI, and Lqp have been determined from Eq. (1), (2), and (3), respectively, using Newton-Raphson load flow data for 'k=0.5' that has been obtained via MATLAB/PSAT and is presented in Table 3. Table 3 shows that all of the indices for the lines (5-1), (3-4), (14-13), (3-2), and (2-4) have exceptionally high values under the base case. Thus, these lines can be regarded as the most severe. Additionally, it is noted that line (5-1)'s FVSI index value is greater than unity, indicating that this line is in a critical state. With the installation of the solar PV generation system, the line indices were once more determined using Eq. (1), (2), and (3) with 'k=0.5', as shown in Table 3. The most severe line (5-1)'s Lmn, FVSI, and Lqp indices improve from 0.9924 p.u. to 0.9816 p.u., from 1.0161 p.u. to 0.9725 p.u., and from 0.9692 p.u. to 0.8297 p.u., respectively, according to this table. Figure 6 displays a bar graph of the line stability indices for the top five severe lines at loading multiplier 'k=0.5'.

4.1.3 Line Stability Indices under PV integration with k=1.0

Lines (5-1), (3-4), (14-13), (3-2), and (8-7) are found to be the top five most severe lines under k=1.0. Under this loading scenario, the FVSI index value (1.0218 p.u.) for line (5-1) shows an unstable condition of this line without integration of the solar PV generation system. After the integration of the solar PV generation system with the IEEE 14-bus system, the line indices value gets reduced; hence, the severity of these severe lines gets reduced as shown in Table 4. A bar graph of the line stability indices for the top five severe lines at loading multiplier 'k=1.0' has been presented in Fig. 7.

4.1.4 Line Stability Indices under PV integration with k=1.2

The top five lines with the highest severity under k=1.2 are determined to be (5-1), (3-4), (14–13), (3-2), and (8–7). The line (5-1)'s FVSI index value (1.0225 p.u.) under this loading scenario indicates that the line is unstable in the absence of a solar PV generation system integration. As demonstrated in Table 5, following the integration of the solar PV generation system with the IEEE 14-bus system, the line indices value decreases and, consequently, does the severity of these problematic lines. Figure 8 shows a bar graph of the line stability indices for the top five severe lines at loading multiplier "k=1.2".

4.2 IEEE 118-Bus System

The standard IEEE 118-bus system has also been used to test and evaluate the suggested approach for evaluating voltage stability [38]. According to the material currently in publication [40], bus number 22 was determined to be the most severe bus in the IEEE 118-bus system. Therefore, this bus can be selected as the most suitable site for the deployment of the compensating devices in the IEEE 118-bus system. In order to improve the system's line voltage stability, a solar PV generation equipment has been installed at bus number 22. The load and generation information of system system is shown in Tab. 6.

4.2.1 Line Stability Indices under PV integration with k=1.0

As seen in Table 7, the line indices Lmn, FVSI, and Lqp values have been calculated using load flow data for every line. Only the twenty most severe lines' line index values are displayed in this table. When solar PV generation is integrated into the system, the Lmn/FVSI/Lqp indices for

***Table 7**: Line stability indices with and without deployment of the solar PV system at loading multiplier k=1.0.*

Lines		Line stability indices (in p.u.) at k=1.0					
From Bus	To Bus	Without PV integration			With PV integration		
		Lmn Indices	FVSI Indices	Lqp Indices	Lmn Indices	FVSI Indices	Lqp Indices
44	**43**	**1.0932**	**0.9408**	**0.9936**	**0.7692**	**0.9048**	**0.9121**
68	**69**	**1.0517**	**0.7902**	**0.9877**	**0.7764**	**0.5878**	**0.5885**
70	**69**	**1.0124**	**0.8978**	**0.9681**	**0.7464**	**0.3929**	**0.6527**
38	**37**	**0.9872**	**0.908**	**0.9534**	**0.8958**	**0.3292**	**0.4628**
70	**24**	**0.9825**	**0.9215**	**0.9738**	**0.3627**	**0.3184**	**0.9141**
74	70	0.9321	0.2103	0.6529	0.9193	0.1232	0.4751
65	66	0.8885	0.7528	0.9262	0.8152	0.6588	0.7705
22	21	0.8784	0.3516	0.1307	0.0131	0.0106	0.1005
59	56	0.8721	0.5762	0.3075	0.3714	0.423	0.0486
66	62	0.8674	0.7691	0.9326	0.1561	0.5681	0.3441
9	8	0.8546	0.5721	0.7334	0.5509	0.5084	0.0148
59	56	0.8468	0.5632	0.3181	0.7438	0.4094	0.0363
30	17	0.7583	0.6333	0.3552	0.5194	0.5796	0.1085
46	45	0.7014	0.5706	0.4867	0.6216	0.4035	0.448
75	69	0.6663	0.2544	0.9267	0.5824	0.1659	0.8221
20	19	0.5887	0.6371	0.5698	0.4653	0.6098	0.5215
43	34	0.5689	0.5941	0.4273	0.5548	0.5158	0.3292
21	20	0.5171	0.4457	0.8801	0.3706	0.3188	0.1172
75	70	0.3926	0.192	0.8555	0.3045	0.1553	0.7162
47	46	0.1494	0.2093	0.5988	0.1147	0.137	0.3392

***Table 8**: Line stability indices with and without deployment of the solar PV system at loading multiplier k=1.2.*

Lines		Line stability indices (in p.u.) at k=1.2					
From Bus	To Bus	Without PV integration			With PV integration		
		Lmn Indices	FVSI Indices	Lqp Indices	Lmn Indices	FVSI Indices	Lqp Indices
44	**43**	**1.2155**	**0.9781**	**0.9815**	**0.9804**	**0.8815**	**0.3904**
38	**37**	**1.0815**	**0.9134**	**0.9647**	**0.8204**	**0.3334**	**0.7546**
68	**69**	**1.0249**	**0.8718**	**0.9813**	**0.7019**	**0.4145**	**0.5547**
70	**69**	**1.0175**	**0.9574**	**0.9576**	**0.8104**	**0.4014**	**0.7014**
70	**24**	**0.9643**	**0.9173**	**1.0021**	**0.6116**	**0.5559**	**0.2948**
74	70	0.9346	0.3143	0.8794	0.8301	0.2048	0.4248
65	66	0.9314	0.7614	0.9517	0.8211	0.6643	0.5116
43	34	0.8815	0.8543	0.8037	0.8011	0.7716	0.7213
9	8	0.8726	0.6011	0.7849	0.4016	0.5349	0.0841
22	21	0.8612	0.3514	0.1717	0.0117	0.0176	0.1453
59	56	0.8601	0.5603	0.4305	0.6208	0.4719	0.0483
66	62	0.8597	0.8316	0.9211	0.3524	0.5334	0.3025
59	56	0.8482	0.5548	0.4212	0.6445	0.4403	0.0349
20	19	0.8345	0.8046	0.7547	0.514	0.6016	0.3842
46	45	0.7918	0.8112	0.5701	0.4776	0.7112	0.2247
30	17	0.7728	0.67914	0.4715	0.3445	0.6246	0.01843
47	46	0.7518	0.4143	0.9641	0.5316	0.1467	0.8914
75	69	0.6849	0.0189	0.9143	0.6014	0.0121	0.8017
21	20	0.5734	0.5198	0.9306	0.2701	0.2246	0.1014
75	70	0.3694	0.4012	0.9608	0.3319	0.2714	0.7234

each line are also evaluated. The values of these indices can be used to determine the severe lines. The top five severe lines at 100% system loading are found to be (44–43), (70–69), (70–24), (38–37), and (68–69). Among these lines, line (44-43) is the most critical line as all its index values are the highest and near unity. For the IEEE 118-bus system, it is found that the integration of solar PV generation at bus number 22 results in a decrease in the line stability index Lmn/FVSI/Lqp. Figure 9 shows a bar graph of the line stability indices for the top five severe lines at loading multiplier ”k=1.0”.

4.2.2 Line Stability Indices under PV integration with k=1.2

The line stability index of the IEEE 118-bus system has been calculated using line flow data under a heavy loading scenario (k = 1.2). From Table 8, it is found that the lines (44-43), (38–37), (68–69), (70–69), and (70–24) have the highest values of line indices. Therefore, these lines can be considered the most severe lines of the system under the loading scenario “k=1.2”. After integrating the solar PV system on the most severe bus number 22, the line severity of the most severe line (44-43) gets reduced from 1.2155 p.u., 0.9781 p.u., and 0.9815 p.u. to 0.9804 p.u., 0.8815 p.u., and 0.3904 p.u. for line

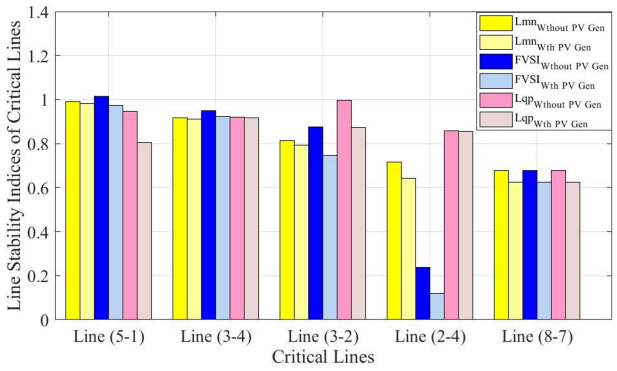

***Fig. 8**: Bar graph of the line stability indices of the most severe lines at loading multiplier k=1.2.*

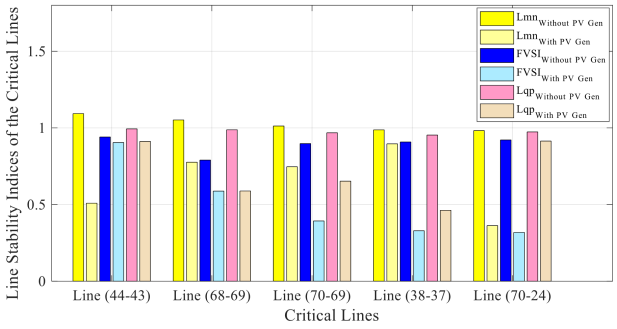

***Fig. 9**: Bar graph of the line stability indices of the most severe lines at loading multiplier k=1.0.*

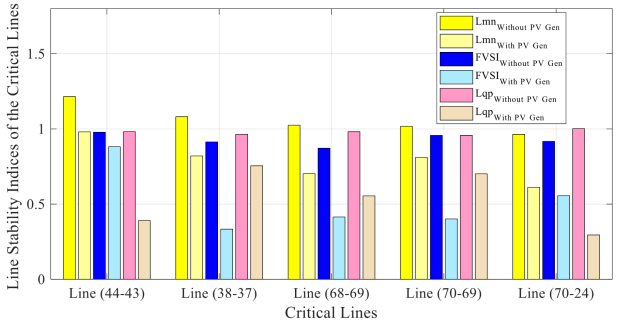

***Fig. 10**: Bar graph of the line stability indices of the most severe lines at loading multiplier k=1.2.*

indices Lmn/FVSI/Lqp, respectively. The bar graph of line stability indices of the top five most severe lines under the loading scenario "k=1.2" for the IEEE 118-bus system is shown in Fig. 10.

5. CONCLUSION

The line stability indices Lmn/FVSI/Lqp of every line in the IEEE 14-bus system have been computed in this work, both with and without the solar photovoltaic system installed. The index value close to unity is used to determine the most severe line. To decrease the lines' severity, the solar system has been connected to the system's critical bus. Under four different load patterns (k = 0.2, 0.5, 1.0, and 1.2), the line stability indices of the lines have been tested with and without the appropriate placement of the solar PV system. The photovoltaic system has been installed on bus 14 in the IEEE 14-bus system. it is observed that the values of the indices Lmn/FVSI/Lqp index for the line (5-1) are higher than other line indices under all four considered types of loading scenarios (k = 0.2, 0.5, 1.0, and 1.2). With the installation of a solar PV system, the values of the indices Lmn/FVSI/Lqp for the line (5-1) get reduced as shown in Tables 2, 3, 4, and 5. Hence, the severity of the most severe line is reduced under all considered load patterns. The effect of the solar PV system on line severity can also be seen from Figures 3, 4, 5, and 6. From these Figures, it is also observed that the values of all line indices get reduced after the integration of the solar PV system at bus 14. In the future, multiple renewable energy sources like wind and solar can be used simultaneously to reduce the higher degree of severity of the most severe lines and enhance the system's loadability.

REFERENCES

[1] C. Vournas, "Power System Voltage Stability," in *Encyclopedia of Systems and Control*, T. Baillieul John and Samad, Ed., London: Springer London, 2013, pp. 1–7. doi: 10.1007/978-1-4471-5102-9_263-1.

[2] A. Jalali and M. Aldeen, "Improving voltage stability margin using STATCOM-storage devices," in *2016 IEEE PES Innovative Smart Grid Technologies Conference Europe (ISGT-Europe)*, IEEE, Oct. 2016, pp. 1–6. doi: 10.1109/ISGTEurope.2016.7856185.

[3] M. Klein, G. J. Rogers, S. Moorty, and P. Kundur, "Analytical investigation of factors influencing power system stabilizers performance," *IEEE Transactions on Energy Conversion*, vol. 7, no. 3, pp. 382–390, 1992, doi: 10.1109/60.148556.

[4] P. Kundur, J. Paserba, V. Vittal, and G. Andersson, "Closure of 'Definition and Classification of Power System Stability,"' *IEEE Transactions on Power Systems*, vol. 21, no. 1, pp. 446–446, Feb. 2006, doi: 10.1109/TPWRS.2005.861952.

[5] M. A. Mostafa, M. E. El-Hawary, G. A. N. Mbamalu, M. M. Mansour, K. M. El-Nagar, and A. N. El-Arabaty, "Steady-state load shedding schemes: a performance comparison," *Electric Power Systems Research*, vol. 38, no. 2, pp. 105–112, 1996, doi: https://doi.org/10.1016/S0378-7796(??)01068-1.

[6] D. Hazarika and A. K. Sinha, "Method for optimal load shedding in case of generation deficiency in a power system," *International Journal of Electrical Power & Energy Systems*, vol. 20, no. 6, pp. 411–420, 1998, doi: https://doi.org/10.1016/S0142-0615(??)00061-6.

[7] M. Z. El-Sadek, G. A. Mahmoud, M. M. Dessouky, and W. I. Rashed, "Optimum load shedding for avoiding steady-state voltage instability," *Electric Power Systems Research*, vol. 50, no. 2, pp.

119–123, 1999, doi: https://doi.org/10.1016/S0378-7796(**??**)00124-2.

[8] M. M. Aman, G. B. Jasmon, H. Mokhlis, and A. H. A. Bakar, "Optimal placement and sizing of a DG based on a new power stability index and line losses," *International Journal of Electrical Power & Energy Systems*, vol. 43, no. 1, pp. 1296–1304, 2012, doi: https://doi.org/10.1016/j.ijepes.2012.05.053.

[9] M. Chakravorty and D. Das, "Voltage stability analysis of radial distribution networks," *International Journal of Electrical Power & Energy Systems*, vol. 23, no. 2, pp. 129–135, 2001, doi: https://doi.org/10.1016/S0142-0615(**??**)00040-5.

[10] V. Balamourougan, T. S. Sidhu, and M. S. Sachdev, "Technique for online prediction of voltage collapse," *IEE Proceedings - Generation, Transmission and Distribution*, vol. 151, no. 4, p. 453, 2004, doi: 10.1049/ip-gtd:20040612.

[11] Y. Song, D. J. Hill, and T. Liu, "State-in-mode analysis of the power flow Jacobian for static voltage stability," *International Journal of Electrical Power & Energy Systems*, vol. 105, pp. 671–678, 2019, doi: https://doi.org/10.1016/j.ijepes.2018.09.012.

[12] Y. Wang, W. Li, and J. Lu, "A new node voltage stability index based on local voltage phasors," *Electric Power Systems Research*, vol. 79, no. 1, pp. 265–271, 2009, doi: https://doi.org/10.1016/j.epsr.2008.06.010.

[13] M. H. Haque, "Use of local information to determine the distance to voltage collapse," in *2007 International Power Engineering Conference (IPEC 2007)*, 2007, pp. 407–412.

[14] U. Sultana, A. B. Khairuddin, M. M. Aman, A. S. Mokhtar, and N. Zareen, "A review of optimum DG placement based on minimization of power losses and voltage stability enhancement of distribution system," *Renewable and Sustainable Energy Reviews*, vol. 63, pp. 363–378, 2016, doi: https://doi.org/10.1016/j.rser.2016.05.056.

[15] M. Moghavvemi and F. M. Omar, "Technique for contingency monitoring and voltage collapse prediction," *IEE Proceedings: Generation, Transmission and Distribution*, vol. 145, no. 6, pp. 634–640, 1998, doi: 10.1049/IP-GTD:19982355.

[16] A. MOhamed, G. Jasmon, and S. Yusof PTI Asia Sdn Bti, "A STATIC VOLTAGE COLLAPSE INDICATOR USING LINE STABILITY FACTORS," *Journal of Industrial Technology*, vol. 7, no. 1, pp. 73–85, 1998.

[17] I. Musirin and T. K. Abdul Rahman, "Novel fast voltage stability index (FVSI) for voltage stability analysis in power transmission system," in *Student Conference on Research and Development*, 2002, pp. 265–268. doi: 10.1109/SCORED.2002.1033108.

[18] W. H. Tang *et al.*, "A composite voltage stability index for integrated energy systems based on L-index and the minimum eigenvalue of reduced Jacobian matrix," *International Journal of Electrical Power & Energy Systems*, vol. 141, p. 108136, Oct. 2022, doi: 10.1016/j.ijepes.2022.108136.

[19] S. Khunkitti *et al.*, "A comparison of the effectiveness of voltage stability indices in an optimal power flow," *IEEJ Transactions on Electrical and Electronic Engineering*, vol. 14, no. 4, pp. 534–544, Apr. 2019, doi: 10.1002/tee.22836.

[20] M. Wang and J. V Milanović, "Simultaneous Assessment of Multiple Aspects of Stability of Power Systems With Renewable Generation," *IEEE Transactions on Power Systems*, vol. 39, no. 1, pp. 97–106, 2024, doi: 10.1109/TPWRS.2023.3241862.

[21] K. D. Dharmapala, A. Rajapakse, K. Narendra, and Y. Zhang, "Machine Learning Based Real-Time Monitoring of Long-Term Voltage Stability Using Voltage Stability Indices," *IEEE Access*, vol. 8, pp. 222544–222555, 2020, doi: 10.1109/ACCESS.2020.3043935.

[22] X. Jia *et al.*, "Static Voltage Stability Assessment Considering Impacts of Ambient Conditions on Overhead Transmission Lines," *IEEE Trans Ind Appl*, vol. 58, no. 6, pp. 6981–6989, 2022, doi: 10.1109/TIA.2022.3195974.

[23] S. Khunkitti, A. Siritaratiwat, and S. Premrudeepreechacharn, "A Many-Objective Marine Predators Algorithm for Solving Many-Objective Optimal Power Flow Problem," *Applied Sciences*, vol. 12, no. 22, p. 11829, Nov. 2022, doi: 10.3390/app122211829.

[24] S. Khunkitti, S. Premrudeepreechacharn, and A. Siritaratiwat, "A Two-Archive Harris Hawk Optimization for Solving Many-Objective Optimal Power Flow Problems," *IEEE Access*, vol. 11, pp. 134557–134574, 2023, doi: 10.1109/ACCESS.2023.3337535.

[25] P. Kessel and H. Glavitsch, "Estimating the Voltage Stability of a Power System," *IEEE Transactions on Power Delivery*, vol. 1, no. 3, pp. 346–354, 1986, doi: 10.1109/TPWRD.1986.4308013.

[26] C. Li *et al.*, "Optimal allocation of multi-type FACTS devices in power systems based on power flow entropy," *Journal of Modern Power Systems and Clean Energy*, vol. 2, no. 2, pp. 173–180, 2014, doi: 10.1007/s40565-014-0059-x.

[27] Z. A. Kamaruzzaman and A. Mohamed, "Impact of grid-connected photovoltaic generator using P-V curve and improved voltage stability index," in *2014 IEEE International Conference on Power and Energy (PECon)*, 2014, pp. 196–200. doi: 10.1109/PECON.2014.7062440.

[28] W. Suampun, "Voltage Stability Analysis of Grid-connected Photovoltaic Power Systems Using CPFLOW," *Procedia Comput Sci*, vol. 86, pp. 301–304, 2016, doi: https://doi.org/10.1016/j.procs.2016.05.082.

[29] B. Tamimi, C. Cañizares, and K. Bhattacharya, "System Stability Impact of Large-Scale and Distributed Solar Photovoltaic Generation: The Case of Ontario, Canada," *IEEE Trans Sustain En-*

ergy, vol. 4, no. 3, pp. 680–688, 2013, doi: 10.1109/TSTE.2012.2235151.

[30] B. B. Adetokun, J. O. Ojo, and C. M. Muriithi, "Reactive Power-Voltage-Based Voltage Instability Sensitivity Indices for Power Grid With Increasing Renewable Energy Penetration," *IEEE Access*, vol. 8, pp. 85401–85410, 2020, doi: 10.1109/ACCESS.2020.2992194.

[31] B. Guddanti, J. R. Orrego, R. Roychowdhury, and M. S. Illindala, "Sensitivity Analysis Based Identification of Key Parameters in the Dynamic Model of a Utility-Scale Solar PV Plant," *IEEE Transactions on Power Systems*, vol. 37, no. 2, pp. 1340–1350, Mar. 2022, doi: 10.1109/TPWRS.2021.3101466.

[32] M. H. Ibrahim, S. P. Ang, M. N. Dani, R. Petra, and M. A. Salam, "Voltage stability assessment for solar photovoltaic penetration using Reactive Power–Voltage and Active Power–Voltage modal analysis," *Energy Reports*, vol. 9, pp. 486–493, 2023, doi: https://doi.org/10.1016/j.egyr.2023.05.124.

[33] D. R. Shrivastava *et al.*, "A novel synchronized data-driven composite scheme to enhance photovoltaic (pv) integrated power system grid stability," *Energy Reports*, vol. 11, pp. 895–907, 2024, doi: https://doi.org/10.1016/j.egyr.2023.12.029.

[34] Y. Kırçiçek and A. Aktaş, "Design and implementation of a new adaptive energy management algorithm capable of active and reactive power control for grid-connected PV systems," *Ain Shams Engineering Journal*, vol. 14, no. 12, p. 102220, Dec. 2023, doi: 10.1016/j.asej.2023.102220.

[35] R. Singh, G. F. Alapatt, and A. Lakhtakia, "Making Solar Cells a Reality in Every Home: Opportunities and Challenges for Photovoltaic Device Design," *IEEE Journal of the Electron Devices Society*, vol. 1, no. 6, pp. 129–144, Jun. 2013, doi: 10.1109/JEDS.2013.2280887.

[36] C. J. Rhodes, "Solar Energy: Principles and Possibilities," *Sci Prog*, vol. 93, no. 1, pp. 37–112, Mar. 2010, doi: 10.3184/003685010X12626410325807.

[37] G.-S. Szabó, R. Szabó, and L. Szabó, "A Review of the Mitigating Methods against the Energy Conversion Decrease in Solar Panels," *Energies (Basel)*, vol. 15, no. 18, p. 6558, Sep. 2022, doi: 10.3390/en15186558.

[38] "IEEE 14-bus and IEEE 118-bus systems," https://labs.ece.uw.edu/pstca/.

[39] S. K. Gupta and S. K. Mallik, "Enhancement in Voltage Stability Using FACTS Devices Under Contingency Conditions," *Journal of Operation and Automation in Power Engineering*, vol. 12, no. 4, pp. 365–378, 2024, doi: 10.22098/joape.2023.11569.1864.

[40] S. K. Gupta and S. K. Mallik, "Voltage Stability Assessment of Power System Using Line Indices with Wind System and Solar Photovoltaic Generation Integration," *Journal of Operation and Automation in Power Engineering*, vol. 13, no. 4, pp. 303–314, 2025, doi: 10.22098/joape.2024.13429.2028.

Santosh Kumar Gupta did B.Tech. in Electrical Engineering from BBDNITM, Lucknow-226028, U.P. in 2012, India, and M.Tech. in Power System from NIT Kurukshetra-136119 in 2014, Haryana, India, and Ph.D from National Institute of Technology, Patna-800005, Bihar, India in 2024. Currently, he is working as Assistant Professor (EE) (Senior Scale) at Government Engineering College, Siwan, Bihar – 841226 under the Department of Science, Technology and Technical Education, Patna, Bihar.

Vikash Kumar He completed his Bachelor's in 2010. Thereafter, he completed his Masters's from BIT, Sindri in 2013 and completed Ph.D. from NIT Patna in 2025. Presently, he is working as an Assistant Professor (Senior Scale) (Electrical Engineering) in Rashtrakavi Ramdhari Singh Dinkar College of Engineering, Begusarai, under the Department of Science, Technology and Technical Education, Patna, Bihar. His research areas include long-term load forecasting, Power System stability, and Smart grid.

Kanchan Bala received the B.E. degree in Computer Science and Engineering (CSE) from Rajasthan University, M.Tech degree in Computer Science from Banasthali University, Jaipur, Rajasthan, and Ph.D from Birla Institute of Technology, Mesra, Ranchi. She is working as Assistant Professor (CSE) at Gaya College of Engineering, Gaya, Bihar – 823003, India, under the Department of Science, Technology and Technical Education, Patna, Bihar.

Shahzad Ahsan He received his B.E. degree in Electrical Engineering from JECRC, Jaipur, India, in 2009, and his M.Tech. degree in Power Systems from Jamia Millia Islamia (JMI), New Delhi, India, in 2012. He served as an Assistant Professor (on contract) at the National Institute of Technology (NIT), Patna, India, from 2014 to 2015. From 2015 to 2017, he was the Managing Director and Co-founder of Himmel Infratech Pvt. Ltd. and also worked as a Guest Faculty in the Faculty of Engineering and Technology, JMI, New Delhi. He is currently serving as an Assistant Professor in the Department of Electrical Engineering at Muzaffarpur Institute of Technology (MIT), Muzaffarpur, India. His research interests include renewable energy systems, photovoltaic power generation, microgrids, power electronics, and Signal processing and filtering.

Ashwini Tiwari received his B.Tech degree in Civil Engineering from HBTI Kanpur in 2012, and his M.Tech. degree from IIT Kanpur in 2015. Currently, he is working as Assistant Professor in the Department of Civil Engineering at L.D.A.H. Rajkiya Engineering College, Mainpuri, Uttar Pradesh – 205119, India.

Zafar Ayub Ansari received B.Tech degree in Electrical Engineering from Aligarh Muslim University, Aligarh in 2009, M.Tech degree in Instrumentation & Control from Aligarh Muslim University, Aligarh in 2011, and Ph.D. degree in Control Systems from NIT, Patna in 2025. Currently, I am working as an assistant professor at LNJPIT Chapra under the Department of Science, Technology and Technical Education, Patna, Govt. of Bihar. My current research focuses on control and optimization of frequency and voltage in a renewable power system.

Dhananjay Kumar received his Bachelor of Engineering degree from Lakshmi Narain College of Technology, Bhopal, Madhya Pradesh, India in 2014, the M.Tech (Electrical Drives) degree from Maulana Azad National Institute of Technology, Bhopal, India in 2017, and the Ph.D degree from Department of Electrical Engineering, Maulana Azad National Institute of Technology, Bhopal, India in 2022. From 2022 to 2023, he worked as a Senior Technologist in the Department of Industrial Research Design and Development (IRDD), Aartech Solonics Ltd., Mandideep, India. Currently, he is working as an Assistant Professor in the Department of Electrical Engineering and Head of Department at Government Engineering College, Siwan, India. He has published more than 60 papers in journals and conference proceedings. His fields of interest are multilevel inverters, Solar PV controllers, power electronics for renewable energy, and energy storage systems.

Ashish Ranjan did B.Tech. in Electrical & Electronics Engineering from School of Engineering, Cochin University of Science and Technology, Kochi, Kerala, India-682022, and M.Tech. in Power System from Delhi Technological University, Delhi, India-110042, and Ph.D from Electrical Engineering Department of NIT Patna. He is currently an Assistant Professor at Senior Scale with the Department of Electrical & Electronics Engineering at Nalanda College of Engineering, Chandi, District-Nalanda, Bihar-803108, India.

Arjun Kumar received his B.Tech in 2010 and M.Tech in 2012 in electrical engineering from B.C.E. Bhagalpur, Bihar, India, and the Indian Institute of Technology, Roorkee, Uttarakhand, India, respectively, and is pursuing a Ph.D. from NIT Patna. He has been working as an assistant professor in the Department of Electrical Engineering at Shri Phanishwar Nath Renu Engineering College in Araria, Bihar, India, since 2021. His research interests include power electronics applications to renewable energy systems, smart grids, solar photovoltaic systems, etc.